Estimation and Modeling of Parameters for Direct Reduction in Iron Ore/Coal Composites: Part II. Kinetic Parameters

E. DONSKOI, D.L.S. McELWAIN, and L.J. WIBBERLEY

The published approaches to the mathematical modeling of rates of reduction, of coal gasification, and of devolatilization of coal in iron/ore coal composites are reviewed and critically analyzed. The effect of different parameters on the overall process is discussed. The concepts of a local rate of reduction and gasification and an integrated rate of reduction are introduced, and the rate-controlling steps in each are reviewed. Current approaches to modeling coal pyrolysis are also described. This review, with the estimates, data, and analysis related to modeling rates of reduction, gasification, and pyrolysis, should prove useful to researchers developing models of coal-based iron ore reduction and related processes.
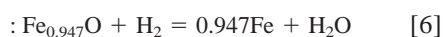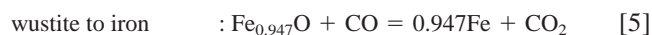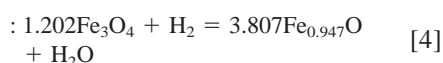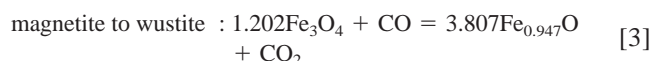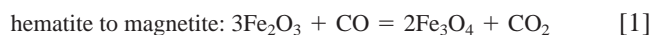
I. INTRODUCTION

The direct reduction of iron ore/coal composites (DRIOCC) is a relatively new coke-free technology which now comprises a small but growing part of the worldwide direct reduction of iron ore industry.

Mathematical models are proving useful in understanding the laboratory experiments and in extrapolating these to the pilot and plant scale. Modeling allows the prediction of the time course of the reduction and may suggest strategies for the overall improvement of the process. The validity of these models depends critically on accurate estimates of the kinetic parameters associated with the iron ore reduction process and the production and consumption of reductants.

This article gives estimates of the relevant kinetic data and provides a critical analysis of models of the rates of iron ore reduction and the gasification of the carbonaceous material used to supply the reductants, as well as a review of several recent models of pyrolysis.

The main reactions for the coal-based direct reduction can be summarized by the following scheme (for details, refer to the article by Donskoi and McElwain[1]):
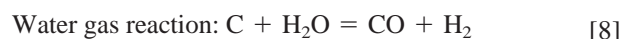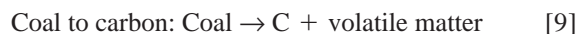
hematite to magnetite: $3Fe_2O_3 + CO = 2Fe_3O_4 + CO_2$ [1]

$: 3Fe_2O_3 + H_2 = 2Fe_3O_4 + H_2O$ [2]

magnetite to wustite $: 1.202Fe_3O_4 + CO = 3.807Fe_{0.947}O + CO_2$ [3]

$: 1.202Fe_3O_4 + H_2 = 3.807Fe_{0.947}O + H_2O$ [4]

wustite to iron $: Fe_{0.947}O + CO = 0.947Fe + CO_2$ [5]

$: Fe_{0.947}O + H_2 = 0.947Fe + H_2O$ [6]

Carbon gasification:

Boudouard reaction: $C + CO_2 = 2CO$ [7]

Water gas reaction: $C + H_2O = CO + H_2$ [8]

Coal devolatilization:

Coal to carbon: Coal $\rightarrow$ C + volatile matter [9]

Various different conditions can prevail during the coal-based iron ore reduction: different specimen and particle sizes, ambient atmospheres, heating regimes, geometries, and compositions. This article reviews and analyzes different approaches to the modeling of kinetic parameters in DRIOCC. It is shown that while the modeling may not necessarily involve all the details of the reaction mechanism, it is still able to adequately represent the overall time course of the reduction.

II. RATE OF REDUCTION

A. Integrated Rate of Reduction

Here we introduce the term "integrated rate of reduction" (IRoR), by which is meant the total rate of reduction of a whole specimen, which may be, for example, a spherical or cylindrical pellet or packed bed. The IRoR does not carry information about the difference between reduction rates at distinct points in the specimen. In the next section, we discuss modeling of the local rate of reduction (LRoR). We note that the IRoR can be regarded as an LRoR if, for example, a large system like a shaft furnace containing pellets with a known IRoR for such pellets is being modeled.

Several authors have studied various aspects of the dependence of the IRoR on process parameters. Table I gives a modified and significantly extended version of the table given by Sun[2] of different experiments on direct reduction by carbonaceous materials.

A number of authors[3–6,8,9] have shown that increasing the amount of carbonaceous materials relative to iron oxide content increases the IRoR. The IRoR also increases with decreasing carbonaceous-material particle size[4,5,9] and with decreasing iron ore particle size.[8,10] As expected, the IRoR has a strong dependence on the type of carbonaceous

Table I. Published Work on Direct Reduction by Carbonaceous Materials (Extended and Modified Version of Table Given by Sun[2])

References		Ghosh and Tiwary[3]	Rao[4]	Fruehan[5]	Srinivasan and Lahiri[6]	Seaton et al.[7]	Otsuka and Kunii[8]
Ore	form	hematite ore	hematite powder	hematite powder, FeO	hematite ore	hematite, magnetite ore	hematite powder
	size, mesh	−60	−325	−200	−300	80 pct pass −325	−100 to 325
Carbonaceous material	form	lignite coke	amorphous carbon	graphite, coal char, charcoal, coke	graphite	coal char	graphite
	size, mesh	−60	−48 to −325	−200	−300	−325	−65 to −325
Specimen	Oxide to carbon material ratio	85/15 to 65/35 by wt pct	1/1.5 to 1/9 by mole	hematite 84/16, wustite 87.5/12.5 by wt pct DAF	1/3 to 1/8 by mole	magnetite 82.8/17.2, hematite 80.4/19.6 by wt pct	80/20 by wt pct
	form	pellets	pellets	pellets packed bed	pellets	pellets	packed bed
	size (mm)	19.1 diameter	7.9 × 12.7 diameter	pellet diameter 6 × 6 to 14 × 14, packed bed depth 5 to 20	diameter 9 to 12	14 diameter	diameter 16 × 20
Temperature, °C		900 to 1100	850 to 1087	900 to 1200	927 to 1060	800 to 1200	1050 to 1150
Atmosphere		SG*	Ar	Ar, He	N_2	N_2	N_2
Reduction measurements		weight	weight	micro-balance	micro-balance	weight	micro-balance
Model		AP**	Eqs [11] and [20]	Eq. [14]	AP	Eqs. [11] and [14]	AP
Activation energy (kJ/mole)		average 78.2	301.2	293 to 335	f dependent f 0.2 – 417 0.6 – 285 0.8 – 56	magnetite 159 hematite 125–239	f < 1/3 230, 260, 272 f > 1/3 fines −325 63, 98
Rate controlling steps suggested by authors		FeO reduction	C gasification	C gasification	C gasifications in final stage FeO reduction	C gasification, heat transfer	C gasification f > 1/3 influenced by size Fe₂O₃

material used.[5,9] For example, Fruehan[5] shows that coconut charcoal has the highest reactivity of those carbonaceous materials studied with, in descending order of reactivity, coal char, coke, and the worst being graphite.

Different additives also can significantly affect the IRoR. Rao[4] has shown that Li_2O promotes reduction, while FeS plays an inhibitive role. Otsuka and Kunii[8] show that the IRoR is slower for larger additions of bentonite. Mookherjee et al.[12] show that the IRoR increases in the presence of Na_2CO_3, which is known to catalyze the gasification reaction. A good review of the effect of different additives on iron oxide reduction can be found in the article by Prakash.[16]

Many authors have studied the dependence of the IRoR on specimen size.[5,6,9,14] While Srinivasan and Lahiri[6] found that pellet diameter has a negligible effect on the IRoR (pellet diameter range studied was from 9 to 12 mm), later articles[5,9,14] have clearly shown that the size of the specimen does affect the kinetics and, for certain experimental setups, heat transfer becomes the rate-limiting step.[7,9,14,15]

At different stages of the reduction, the IRoR is different. The dependence of the IRoR on the degree of reduction has been shown by several investigators.[6,8,11,13]

Pressing the specimen can also affect the IRoR. Otsuka and Kunii[8] pressed samples without bentonite, and this gave a much larger IRoR than for the same samples with-

Table I. Continued   Published Work on Direct Reduction by Carbonaceous Materials (Extended and Modified Version of Table Given by Sun[2])

Bruk and Lu[9]	Prakash and Ray[10]	Reddy et al.[11]	Mookherjeee et al.[12]	Haque et al.[13]	Nascimento et al.[14]	Wang et al.[15]
magnetite ore −75 μm	iron ore −10 + 6 mm − 6 + 3 mm	iron ore −150 μm	iron ore −500 μm + 250 μm	iron ore 0.75 to 2.4 mm	iron ore 80 pct under 100 μm	iron ore fines
high volatile, coal, graphite	noncoking coal	coal	coal or coal char	coal	charcoal	hard and soft coal
−75 to −1400 μm	−10 + 6 mm −6 + 3 mm	−150 μm	−500 μm +250 μm	0.75 to 2.4 mm	95 pct under 100 μm	fines
80.7/19.3 to 70/30, wt pct, graphite 84.8/15.2	1:0.6 to 1:1 weight ratio	only fixed carbon 1:0.97 to 1.94 by mole	not mixed 1:1, 1:2 weight ratio	1:0.7 to 1:0.9 weight ratio	1:3 to all carbon in mole	Fixed C to O in iron oxide 1.0
packed bed	packed bed	pellets	iron ore surrounded by carbon material	packed bed	pellets	pellets
diameter 19 to 43 × 90 to 132	85 × 75 diameter	14 diameter	15 × 30 diameter 33 × 50 diameter	30 × 38 diameter	9.1 to 15.3 diameter	16 to 18 diameter
900 to 1300 Ar, air chemical analysis	800 to 1000 SG chemical analysis	900 to 1100 SG weight C left	850 to 1050 SG chemical analysis	950 to 1050 air initial chemical analysis	1000 to 1150 Ar weight	900 to 1300 N₂ weight and chemical analysis
— not discussed	Eq. [22] isothermal reduction 90.9, 111.2 noniso-thermal 72.7 to 75.7	Eq. [19] initial stages 108.2, later 93.2	Eq. [22] f 0.2 to 130.7 0.3 – 152.1 0.6 – 144.7 0.7 – 146.3	Eq. [10] 148 to 151	Eq. [20] for FeO → Fe stage 9.1 mm-146 15.3 mm-91	Eq. [14] initial stage 68.95 to 82.61 later reduction is independent of furnace temperature
heat transfer	not discussed	chemically controlled	C gasification	not discussed	for 9.1 mm heat transfer and C gasification for 15.3 mm heat transfer	initial stage chemical reaction later heat transfer

* Information about the atmosphere has not been given, so the atmosphere assumed to be self-generated.

** The kinetics has been assumed to follow an Arrhenius plots. Fractional reduction (refer to text) per unit time is taken as an empirical rate constant $k = k_0 \exp (-E/RT)$. The basic equation used in $df/dt = k_0 \exp (-E/RT)$, so, to find E (activation energy), plots of $\log_{10} (k)$ or $\ln (k)$ against $1/T$ have been produced.

out pressing. When bentonite was added to the mixture, pressing decreased the reduction rate.

Depending on the reduction temperature and experimental setup, the effect of volatiles can be negligible or quite significant. Dey et al.[17] have drawn the conclusion that, at temperatures below 1000 °C, hematite/noncoking coal pellets are mainly reduced by volatiles, whereas at a higher reduction temperatures, there is a decrease in reduction by gases and an increase in reduction by carbon. Wang et al.[18] show that before the fast reduction by carbon (at about 900 °C), reduction by volatile matter is quite significant. In another investigation,[15] where the temperatures were higher than 1050 °C, they con-

clude that reduction by volatiles was negligible, as they were almost completely released in the initial period of heating. Dutta and Ghosh[19] studied pellets that were heated from room temperature to 1000 °C and concluded that while carbon was the major reductant, reduction by H_2 was also significant.

The surrounding atmosphere also plays a significant role on the IRoR.[20,21] Carvalho et al.[20] studied the effect of various flow rates of different gases (N_2, CO, and CO_2) on composite pellet reduction. They showed that the IRoR dropped with an increasing flow rate of N_2 and associated this with the greater internal dilution of reactive gases. Initial rates of reduction with CO or

CO_2 atmospheres were higher than in an N_2 atmosphere. During the later stages of reduction, as expected, a CO atmosphere promoted reduction, while in a CO_2 atmosphere, the IRoR significantly decreased until reduction practically ceased. Fruehan[5] has shown that the IRoR may increase or decrease with ambient-atmosphere pressure, depending on the form of carbon and the temperature.

As can be seen from the previous review, the rate of reduction is significantly affected by various factors, and there is no technique at present to predict the rate of reduction, even knowing all the primary process parameters, without some experimental measurements.

However, Haque et al.[13] have developed an approach to predict the time (τ_f) for a certain degree of reduction (or IRoR), depending on operating variables. They studied the packed-bed reduction of iron ore fines with coal fines (Table I provides details) and have derived an empirical integrated rate equation describing the relationship between different process variables, namely,

$$\tau_f = 2.92 \times 10^{-5} f^{2.24} m^{-0.94} d^{0.38} h^{0.28} H_{Fe}^{-0.48} H_c^{-0.33}$$
$$\times \exp(150,000/RT) \quad [10]$$

Here, m is the coal/ore ratio in the initial reduction mixture, d is the average ore and coal particle size, h is the bed depth of the mixture, H_{Fe} is reducibility of iron ore, and H_c is reactivity of coal. This equation can be used to estimate the time required for a particular degree of reduction (f) in the range of 0.6 to 0.9, or *vice versa*. It should be noticed that this regression approach is applicable only for a certain range of parameters and conditions studied in their work. The very useful aspect of the model is that it shows the relative importance on the rate of reduction of different parameters in the ranges studied (particle size of 0.75 to 2.4 mm, bed depth of 24 to 38 mm, temperature of 950 °C to 1050 °C, iron ore reducibility of 5.268×10^{-2} to 8.66×10^{-2} kmol O m^{-3} s^{-1}, coal reactivity of 0.728×10^{-3} to 1.473×10^{-3}, and coal ore ratio of 0.7 to 0.9). For example, it can be seen that, for large particles such as those used by the authors, under these conditions, the effect of the reducibility of iron ore is higher than the effect of coal reactivity (the exponent of H_{Fe} is higher than that of H_c in Eq. [10]). It can be concluded that, under these conditions, the reduction of iron oxide is a more critical step than the carbon gasification.

Unfortunately, the accuracy of this regression model has not been estimated. However, the theoretical time-reduction curves for different degrees of reduction fit the overall results quite well (Figure 1).

The most widespread approach to the prediction of the degree of reduction at a certain time in a mixture of iron ore and coal fines is to assume that it is an isothermal system and the reaction is chemically controlled. The following rate equation for a pseudohomogeneous reaction of the first order is used:

$$\frac{dW}{dt} = -KW \quad [11]$$

where K is a rate constant and W can be the weight of carbon (Fruehan[5]) or oxygen left in the mixture or the weight loss (Prakash[22]). Experiments carried out at different
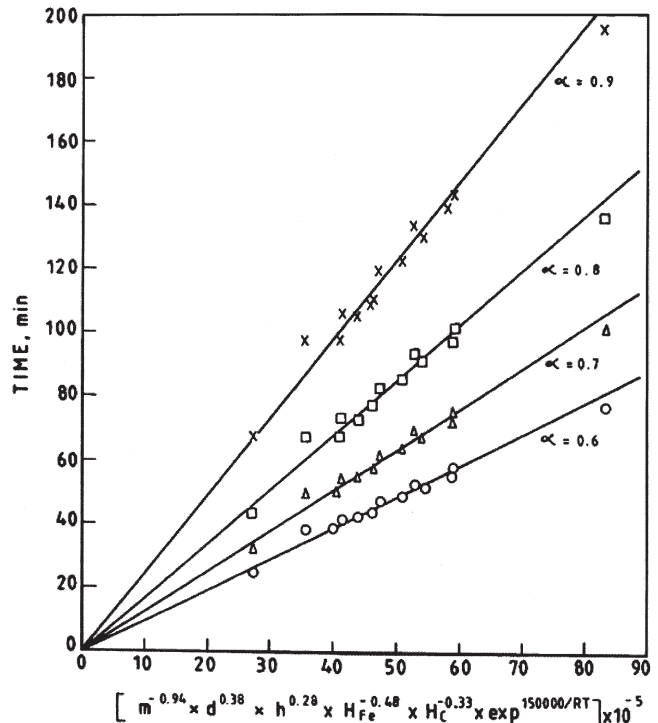

Fig. 1—Correlation for four degrees of reduction (this figure is a reproduction of Figure 7 from Haque et al.[13]).

fixed temperatures allows K to be expressed in Arrhenius form as

$$K = k_0 \exp(-E/RT) \quad [12]$$

where k_0 is the pre-exponential factor, E is the apparent activation energy, R is the ideal gas constant, and T is the absolute temperature.

If the parameter f, showing the fraction of a measured parameter removed from the initial value, is used, Eq. [11] would be expressed as

$$\frac{df}{dt} = K(1 - f) \quad [13]$$

Often an integral form is used, namely,

$$\ln(1 - af) = -Kt \quad [14]$$

where a is a constant close to unity. In the article by Seaton et al.,[7] $a = 0.98$ for hematite and $a = 1.037$ for magnetite, whereas Carvalho et al.[20] and Wang et al.[15] employed $a = 1.0$. Often, f measures the degree of reduction. This can be defined in two different ways. Haque and Ray[23] use an expression for the degree of reduction calculated from a relationship suggested by Chernyshev et al.[24] and Gonzales and Jeffes,[25] namely,

$$f = R_w \frac{\text{pct Fe}_T^r - \text{pct Fe}_T^i}{\text{pct Fe}_T^r \times \text{pct Fe}_T^i} \times 100 \quad [15]$$

where R_w is the ratio of the weight of iron to that of oxygen in the iron ore, pct Fe$_T^r$ is the percentage of total iron in the reduced mass, and pct Fe$_T^i$ is the percentage of total iron in the initial ore.

Sometimes a simpler expression for the degree of reduction is used (as in the article by Reddy et al.[11] for example), namely,

$$\text{Degree of reduction} = \frac{\begin{array}{c}\text{weight of oxygen}\\\text{removed from iron ore}\end{array}}{\begin{array}{c}\text{weight of removable}\\\text{oxygen}\end{array}} \times 100 \quad [16]$$

Reddy et al.[11] developed an approach where direct reduction of iron ore by coal in a pellet is treated as a homogeneous nonelementary reaction. They considered the overall reaction

$$Fe_2O_3 + 1.5C = 2Fe + 1.5CO_2 \quad [17]$$
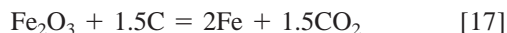
and the rate of this reaction has been expressed by the equation

$$-r_A = -\frac{dC_A}{dt} = kC_A C_B \quad [18]$$

where C_A is the concentration of Fe_2O_3 (mol g^{-1}), C_B is the concentration of fixed carbon (mol g^{-1}), and $-r_A$ is the rate of disappearance of Fe_2O_3. After simple transformations, a kinetic rate equation in terms of molar concentrations of reactants, i.e., iron oxide and carbon in coal, has been derived, namely,

$$\frac{1}{C_{AO}\,(1.5 - M)} \ln \frac{M(1 - X_A)}{(M - 1.5X_A)} = Kt \quad [19]$$

where C_{AO} is initial concentration of Fe_2O_3, M is the ratio of the initial concentrations of carbon to Fe_2O_3, X_A is a fractional conversion of Fe_2O_3, K is a rate constant, and t is time. This equation is valid for $M > 1.5X_A$ and fits the experimental data reasonably well. However, even if the assumption of production of pure carbon dioxide in Reaction [17] is questionable, the model itself is useful. It shows how to estimate the dependence of the rate of the reduction on the initial Fe_2O_3/C ratio. In addition, even though DRIOCC is a heterogeneous reaction, the fact that it can be modeled as a homogeneous nonelementary reaction is important.

Nascimento et al.[14] carried out a kinetic analysis for the FeO → Fe step of the reaction in an iron ore/charcoal composite. The best fit was analogous to the boundary reaction–controlled shrinking-core model,[26,27] namely,

$$1 - (1 - f)^{1/3} = Kt \quad [20]$$

It is interesting to note that the authors showed that, with the same composition but for different pellet sizes, the reaction rates were quite different; they were higher for smaller pellets and lower for larger ones. The apparent activation energy (Eq. [12]) for a 9.1-mm-diameter pellet was 146 kj mol^{-1}, and that for a 15.3-mm pellet was 91 kJ mol^{-1}. We note the effect of heat transfer: the activation energy decreased even though the total reduction rate dropped.

An analogous equation has been used by McAdam et al.[28] for modeling the reduction of ironsand-concentrate pellets containing coal or char and by Rao[4] for modeling the reduction kinetics in an $Fe_2O_3 + 9C$ mixture catalyzed by adding 5 wt pct of Li_2O.

Some authors (Baukloh and Durrer[29] and Yun,[30] for example) have attempted to verify Jander's[27] equation using the Fe_2O_3–C system, namely,

$$(1 - (1 - f)^{1/3})^2 = \frac{Kt}{r^2} \quad [21]$$

where r is the initial radius of the oxide particle and t is the time. A good review of this approach is available in an article by Rao.[4] Dey et al.[17] studied the reduction characteristics of hematite–noncoking coal composite pellets (size of fines from 40 to 80 μm, and 10 mm pellets), and they found that reduction follows mixed kinetic laws which are dependent on temperature as well as on the degree of reduction. The data for 900 °C and 950 °C are fitted well by Jander's model. At 1000 °C and above, and for f values less than 0.5, the data are fitted by a parabolic model ($f \sim t^2$), and for f values greater than 0.5, the data are fitted by Jander's model.

For a mixture of quite large particles (6 to 10 mm), Prakash and Ray[10,31] have reported isothermal kinetic studies showing that DRIOCC in a packed bed follows the Crank–Ginstling–Brounshtein (CGB) kinetic model developed for cases when diffusion through the product layer controls the overall reaction,[27] namely,

$$1 - \frac{2}{3}f - (1 - f)^{2/3} = Kt \quad [22]$$

They also have shown that Eq. [22] is appropriate for a non-linear temperature-time heating program for a moving-bed process. For a process where iron ore fines are surrounded by (not mixed with) coal or char fines, Mookherjee et al.[12] have shown that the degree of reduction of ore as well as the degree of gasification of char both follow the CGB kinetic model.

B. Local Rates of Reduction and Gasification

As discussed earlier, heat transfer can be the rate-limiting step under certain experimental conditions. The difference in the temperature between the center and surface of the specimen can be quite significant, so the LRoR (Reactions [1] through [6]) will be different. The same is true for the LRoG (Reactions [7] and [8]). In Seaton's et al.'s experiment[7] (hematite pellets, 14-mm diameter) for a reduction temperature of 1100 °C, the difference between the center and surface temperature was more than 50 °C for more than 7 minutes, while the reduction took less than 20 minutes. In Huang and Lu's experiment[32] (furnace temperature of 1200 °C and thickness of the cylindrical wall of 35 mm), after 20 minutes, the difference between the outer- and inner-region temperatures was still more than 700 °C.

Even if the temperatures and compositions of the solid components are the same, the LRoR (and, so, the LRoG) can be different if the outer atmospheres are different, especially if forced convection is involved. Carvalho et al.[20] and Ghosh et al.[21] have clearly shown the influence of the ambient atmosphere on the reduction behavior of composite pellets.

The kinetic parameters of the gasification process can be very different, depending on the type of carbonaceous material, the amount and chemical composition of impurities, the reducing atmosphere, particle size, porosity, etc.

The reported values of the activation energy of the gasification reaction vary significantly. Armington[33] reports that the activation energies for gasification of graphitized carbon blacks with CO_2 vary from about 305 to 406 kJ/mol. Ergun[34] reports an activation energy of 234 kJ/mol for three different carbons for the same reaction. For the gasification of graphite granules in CO_2, Turkdogan et al.[35] report a heat of activation of 305 kJ/mol. Even if the gasification kinetics of a certain carbonaceous material is well known, in a mixture with iron ore and other additives, like bentonite or lime, for example, the kinetics can be markedly different.

The significant catalytic effect on the carbon gasification of small amounts of metals and oxides has been extensively investigated.[36–39] Turkdogan and Vinters[39] have shown that the rate of oxidation of graphite impregnated with iron in CO_2–CO mixtures increases by several orders of magnitude over the rate for graphite alone. For charcoal (with 3.5 pct ash, mainly Na_2O, K_2O, Fe_2O_3, Al_2O, and SiO_2) gasification by H_2O, Long and Sykes[40] obtained an activation energy of around 230 kJ/mol, but, after the extraction of impurities, the activation energy was estimated to be about 347 kJ/mol. Fruehan[5] hypothesizes that such a dramatic catalytic effect takes place when the catalyst is impregnated into the carbon, but if there is just simple contact with the carbon, the change of the rate should not be significant. However, if we examine Table I, it can be seen that even when the authors came to the conclusion that the reduction was chemically controlled (for example, the work by Reddy et al.[11] and Wang et al.[15]), the activation energy was much smaller than that reported for the gasification Reactions [7] and [8].

It should be noted that the reduction and gasification processes are cyclically connected. In the Boudouard and water gas carbon gasification reactions, CO_2 and H_2O react with carbon to form carbon monoxide and hydrogen, respectively. Part of these, in turn, react with iron oxides, reducing the amount of oxygen in the iron ore, and produce carbon dioxide and water gas, some of which will react with carbon again. Thus, the reduction and gasification processes are strongly coupled, no matter how the overall reaction is controlled (by the gas-carbon reactions or the gas–iron oxide reactions). This coupling should be explicit when the LRoR and LRoG are modeled. Taking this into account, modeling of the LRoR and LRoG are addressed here in the same section. Different experimental setups can mean that a model must include such effects as heat and mass transfer. Here, we do not discuss all the details of such models, which would include all governing equations and boundary conditions, but focus on modeling the LRoR and LRoG.

Haque et al.[41] modeled the reduction of Khandband iron ore fines ($-2 + 1$ mm) in a mixture with Parascole coal char fines ($-2 + 1$ mm) where the C_{fix}/Fe_T ratio was 0.56. The following information was defined for developing their mathematical model: (1) data on the reduction of iron ore fines by CO; (2) data on the gasification of coal char fines by CO_2; (3) gas equilibrium conditions (equilibrium constants provided in the Appendix) in the system at different temperatures; and (4) isothermal kinetic data for the reduction of iron ore fines by coal char fines.

Haque et al. assume that the reduction of iron ore fines by CO follows Eq. [13], and the final expression for the rate of oxygen removal (V_O) they use is

$$V_O = 4.48 \times 10^{-2} M_{Fe} A_r \exp\left(-E_r/RT\right) \times (1 - f)(1 - p_{CO_2}^o/p_{CO_2}^{eq}) \text{ kg atom/m}^3/\text{s} \quad [23]$$

where M_{Fe} is the amount of iron in the charge, A_r is the reducibility factor of ore (11.44×10^{-3} s^{-1}), E_r is the activation energy for the reduction reaction of iron ore by CO (33 kJ/mol), f is the degree of reduction, $p_{CO_2}^o$ is the actual CO_2 partial pressure in the gas phase, and $p_{CO_2}^{eq}$ is the CO_2 partial pressure in equilibrium with Fe_2O_3–Fe_3O_4–CO or with Fe_3O_4–FeO–CO or with FeO–Fe–CO.

The rate of gasification of coal char by CO_2 was taken to be proportional to the difference between $p_{CO_2}^o$ and $p_{CO_2}^{eq'}$, the CO_2 partial pressure in equilibrium with C and CO, and has been expressed as

$$V_C = (M_C A_R/R'T) \exp\left(-E_g/RT\right) \times (p_{CO_2}^o - p_{CO_2}^{eq'}) \text{ kg atom/m}^3/\text{s} \quad [24]$$

where M_C is the amount of carbon in the charge, A_R is the reactivity factor of coal char (1642 m^3/kgs), R' is the gas constant (m^3 atom/kg mol K), and E_g is the activation energy for the gasification reaction.

To find $p_{CO_2}^o$, the actual CO_2 partial pressure in the gas phase for the reduction of iron ore fines by coal char fines, and the rate of reduction in the mixture, a steady-state assumption has been made, namely, that the CO_2 concentration does not change rapidly, so that the rate of oxygen removal from iron oxide in kg atom/m^3/s is assumed to be equal to the rate of carbon gasification, i.e., $V_O = V_C$. After simple transformations, the expression for the rate of the degree of reduction obtained was

$$\frac{df}{dt} = \frac{C_3 \exp\left(-E_r/RT\right)(1 - f)(1 - p_{CO_2}^{eq'}/p_{CO_2}^{eq})}{1 + C_1 T \exp\left((E_g - E_r)/RT\right)(1 - f)(1/p_{CO_2}^{eq})} \quad [25]$$

where $C_1 = 4.48 \times 10^{-2} M_{Fe} A_r R'/M_C/A_R$, and $C_3 = 1.67 A_r$. From the plots of f against the reduction time and of $-\ln(1 - f)$ against the reduction time, the authors found that the appropriate kinetic equation for the reduction of iron oxide by coal char is the first-order reaction model (Eq. [14] with $a = 1$).

Here, the steady-state assumption means that the reduction and gasification reactions are independent, so that there is no effect of one on the other except through the gaseous intermediates CO and CO_2, and, for the large particles considered ($-2 + 1$ mm), the true direct reduction (solid-solid reaction between carbon in the coal char and iron ore) can be neglected. The steady-state assumption has also been used by Bogdandy and Engel[42] for the reduction of iron ore by coal in a rotary kiln. Although the steady-state assumption appears to be reasonable, the result that $V_O = V_C$ seems to be open to question. It follows, from this expression, that only carbon monoxide is produced. However, it is known that CO_2 is always present and is evolved as well. Let us assume that the partial pressures of these gases are $p_{CO_2}^o$ and p_{CO}^o and that $K_r = p_{CO_2}^o/p_{CO}^o$. Then, the product gaseous mixture is $K_r CO_2 +$

CO, so that for every $(K_r + 1)$ kg atoms of carbon, $(2K_r + 1)$ kg atoms of oxygen are removed. Then, if the total pressure is P, the steady-state assumption would imply that

$$\frac{V_C}{V_O} = \frac{K_r + 1}{2K_r + 1} = \frac{P}{P + p_{CO_2}^o} \qquad [26]$$

In Figure 2, where the authors compare the predicted and experimental reduction results, after approximately half of the reduction, the theoretical curves start to go above the experimental ones, even though in the experiments on gasification of coal char with CO_2, the rate of gasification becomes slower than the predictions after a significant degree of gasification (≈ 0.6 for 957 °C and 0.7 for 1057 °C). We have modeled the reduction process, assuming that relation [26] holds, and the curves started to go even higher than before. This can be seen from the following argument. In expression [26], some carbon dioxide is allowed to be produced, so the gasification reaction, which is rate-limiting in this case, will become even faster. We argue that assumption [26] is more realistic than the assumption that $V_O = V_C$, but the actual reduction of iron ore by coal char is affected by heat transfer, which slows down the reduction and must be taken into account.

In modeling Seatons et al's.[7,43] results for reduction in a highly swelling iron ore–coal char composite pellet, Donskoi and McElwain[1] derive a system of seven differential equations: three equations for the reduction of iron ore (hematite to magnetite, magnetite to wustite, and wustite to iron), one equation for carbon consumption, one equation each for heat transfer and devolatilization of coal, and an equation for size change.

The transitions of hematite (H) to magnetite (M), magnetite to wustite (W), and wustite to iron (F), all measured in kg/m³, are considered to be first-order reactions, and production of these species is given by the following expressions:

$$\frac{dH}{dt} = -Hk_H \exp\left(-E_H/(RT)\right) \qquad [27]$$

$$\frac{dM}{dt} = xHk_H \exp\left(-E_H/(RT)\right) - Mk_M \exp\left(-E_M/(RT)\right) \qquad [28]$$
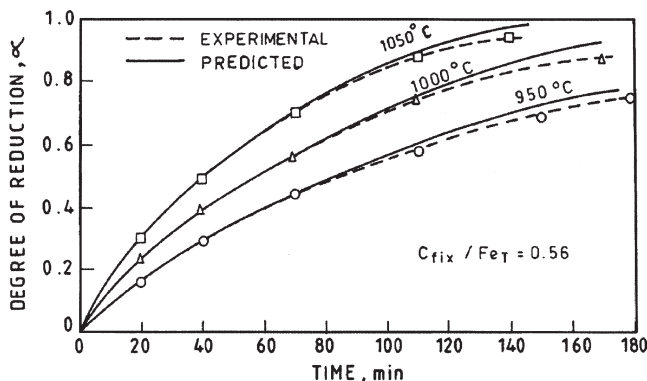

Fig. 2—Comparison of predicted values of degree of reduction with experimental values at different temperatures and times for reduction of iron ore with coal char for $C_{fix}/Fe_T = 0.56$ (this figure is a reproduction of Fig. 15 from Haque et al.[41]).

$$\frac{dW}{dt} = yMk_M \exp\left(-E_M/(RT)\right) - Wk_W \exp\left(-E_W/(RT)\right) \qquad [29]$$

$$\frac{dF}{dt} = zWk_W \exp\left(-E_W/(RT)\right) \qquad [30]$$

where x, y, and z are the weight coefficients; k_H, k_M, and k_W are the apparent frequency factors; and E_H, E_M, and E_W are apparent activation energies, all constant.

The rate of consumption of carbon (C) is modeled as a function of the reduction reaction rates, so that the rates of reduction and the rate of carbon consumption are strongly coupled. The rate of carbon consumption is given by the equation

$$\frac{dC}{dt} = -Q_H Hk_H \exp\left(-E_H/(RT)\right) - Q_M Mk_M \exp \\ \left(-E_M/(RT)\right) - Q_W Wk_W \exp\left(-E_W/(RT)\right) \qquad [31]$$

where Q_H, Q_M, and Q_W are coefficients dependent on weight relationships and equilibrium conditions for a corresponding reaction (Donskoi and McElwain[1] provide details).

The experimental and modeling results agree quite well. Note that the activation energy for the IRoR obtained by Seaton et al.[7] varied from 239 to 125 kJ/mol, while the intrinsic activation energies ($E_H = 380$ kJ/mol, $E_M = 410$ kJ/mol, and $E_M = 330$ kJ/mol) were much higher. Again, we attribute this to the effect of heat transfer.

In earlier work, Donskoi and McElwain[44,45] used an even simpler approach to modeling the LRoR. The reduction process is regarded as a first-order reaction, and the following relationship for the local degree of reduction (f_l) was used:

$$\frac{df_l}{dt} = k_0 \exp\left(-E/RT\right)(1 - f_l) \qquad [32]$$

The rate of carbon consumption (gasification) is assumed to be proportional to the rate of reduction, depending on the stage of reduction and local equilibrium conditions. This approach requires only three equations: Eq. [32] and one each for the heat transfer and for the evolution of pyrolytic matter, if there is any. This model permits the authors to study the effects of nonuniform heating[44] (two-dimensional) and the layering of pellets.[45] However, in this model, only two (major) iron-bearing phases can coexist, while in the previous approach, there can be three or even four. We should note that an X-ray diffraction analysis of the material studied by Seaton et al.[7] demonstrated that up to three different iron-bearing phases may coexist, although one or two phases are in minor quantities.

In these models, heat transfer is the main factor governing the reduction process, but, in general, mass transfer by gaseous species also should be taken into account. This would be important, for example, if the specimen is large or the effect of varying the reduction atmosphere is being investigated.

A model where both heat and mass transfer are taken into account was thoroughly developed in the excellent studies by Sun and Lu.[2,46–48] In the first experiment, Huang and Lu[32] studied reduction in a cylindrically shaped specimen, and Sun and Lu[46] developed a model of this. Later, Sun and Lu[47,48] investigated the reduction

of magnetite iron ore mixed with coal in a packed bed (thickness of 28 mm, ore/coal ratio of 80/20 by weight) and modeled it in a similar manner. The system was described by 19 equations to give local values of the temperature, rates of reactions, composition of solids, pressure, velocity of gas flow, and concentrations of gases.

In these studies, the LRoR is modeled as a sum of the rates of reduction by CO and H_2. The rate of reduction by CO in consecutive reaction "i" is modeled according to the unreacted-core model[27] and is expressed as

$$R_i^{CO} = S_{fi} n_i 4\pi \bar{r}_i^2 k_i^{CO} \left(C_{CO} - \frac{C_{CO_2}}{K_{Ei}^{CO}} \right) \quad [33]$$

where S_{fi} is the shape factor of particles; n_i is the number of particles of solid reactant in the mixture; $\bar{r}_i$ is the average radius of a particle; k_i^{CO} is a rate constant; C_{CO} and C_{CO_2} are the concentrations of CO and CO_2, respectively; and K_{Ei}^{CO} is the equilibrium constant for the i reaction. Here, k_i^{CO} has the Arrhenius-type expression, namely,

$$k_i^{CO} = k_{i0}^{CO} \exp \left(\frac{-\Delta E_{iCO}^*}{RT} \right) \quad [34]$$

where k_{i0}^{CO} and ΔE_{iCO}^* are the pre-exponential factor and activation energy for this reaction, respectively. The rates of reduction by H_2 are modeled with equations analogous to expressions [33] and [34].

The rate of the char gasification is also modeled as a sum of the rates of gasification by the two species CO_2 and H_2O, and the expressions given for them are

$$\dot{R}_c^{CO_2} = S_c n_c 4\pi \bar{r}_c^2 k_c^{CO_2} \left(C_{CO_2} - \frac{C_{CO}^2}{K_{E_c}^{CO_2}} \right) \quad [35]$$

and

$$\dot{R}_c^{H_2O} = S_c n_c 4\pi \bar{r}_c^2 k_c^{H_2O} \left(C_{H_2O} - \frac{C_{CO} \times C_{H_2}}{K_{E_c}^{H_2O}} \right) \quad [36]$$

As can be seen, the rates of reduction and gasification are strongly coupled through the gas concentrations.

Note that care should be taken when the shrinking-core model (SCM) is used. Do[49] showed that for reactions in porous media, the SCM is a special case of the homogeneous model when the time scale for the reaction is much shorter than the time scale for diffusion. Here, we estimate the size of the hematite particles for which application of the SCM is valid. Do gives the following criterion for the reacting porous system to be considered as a shrinking-core system:

$$\phi \gg 1 \quad [37]$$

where ϕ is the shrinking-core reaction modulus, which represents the ratio of the capacities of the shrinking-core system for chemical reaction and for diffusion. Szekely et al.[27] gives this criterion as $\phi > 3$. From Usui et al.,[50] we can get expressions for effective diffusivities and reaction-rate constants obtained on the basis of the SCM.[51] The shrinking-core reaction modulus in this case is

$$\phi^2 = \frac{rk(1 + K_E)}{D_e K_E} \quad [38]$$

where r is the radius of the particle, k is a rate constant for the chemical reaction, K_E is the equilibrium constant, and D_e is an effective diffusivity. From Szekely's expression, the smallest radius (r_{sm}) for which the system will behave as a shrinking core is given by

$$r_{sm} = \frac{9 D_e K_E}{k(1 + K_E)} \quad [39]$$

In the initial step of reduction, when the hematite or magnetite particle is not porous, $D_e \to 0$, so the SCM is applicable even for very small particles. It is possible to develop estimates for further reduction by CO (k is in cm/s, D_e is in cm^2/s):

(1) Magnetite to Wustite

    (a) (1200 K) $K_E = 3.79$, $k = 1.25$, $D_e = 0.14$, $r_{sm} = 0.77$ cm

    (b) (1400 K) $K_E = 6.61$, $k = 2.60$, $D_e = 0.18$, $r_{sm} = 0.55$ cm

(2) Wustite to Iron

    (a) (1200 K) $K_E = 0.44$, $k = 0.82$, $D_e = 0.19$, $r_{sm} = 0.62$ cm

    (b) (1400 K) $K_E = 0.34$, $k = 1.37$, $D_e = 0.26$, $r_{sm} = 0.43$ cm

As can be seen, hematite iron ore particles should be at least 1 cm in diameter for the SCM to be used and for the reaction to be topochemical in nature. In the experiment described in Huang and Lu,[32] 95 pct of the ore particles were less than 0.2 mm. This was the first experiment Sun and Lu modeled. Data regarding the particle size in the second experiment have not been reported. Unfortunately, we cannot find data on magnetite ore to check the validity of the SCM, but the fit to the experimental data in Sun and Lu's study is quite good.

As can be seen from the previous discussion, the more porous the iron ore or the carbon particles are, or the smaller the size of the particles, then the less likely that the SCM is applicable and the less likely reduction is to be of the topochemical type with distinct interfaces. When the SCM approach is not likely to be valid, other modeling approaches should be used: for example, the homogeneous model (Boersma et al.,[52] Dudukovic and Lamba,[53] and King and Jones[54]) or the grain model (Szekely[27]), or the random pore models (Bhatia and co-workers,[55,56,57] for example), although their introduction can significantly complicate the modeling.

Taking into account that many studies (Table I) have shown the validity of an Arrhenius dependence during the reduction process, initially simple expressions for local rates of reduction and gasification such as

$$\dot{R}_i^{CO} = G(f) C_{Fe_i} k_i^{CO} \left(C_{CO} - \frac{C_{CO_2}}{K_{E_i}^{CO}} \right) \quad [40]$$

$$\dot{R}_c^{CO_2} = H(f) C_C k_c^{CO_2} \left(C_{CO_2} - \frac{C_{CO}^2}{K_{E_c}^{CO_2}} \right) \quad [41]$$

should be tried. In these equations, C_{Fe_i} is the concentration of the appropriate iron oxide, and C_C is the concentration of carbon. The k terms have an Arrhenius dependence on the temperature, and $G(f)$ and $H(f)$ are functions of the degree of reduction. These can be determined empirically or obtained from the models mentioned previously. Note that these expressions have the main expected dependencies on the solid reactant concentration, on the gas concentrations, and on the degree of reduction and an Arrhenius dependence on temperature.

III. COAL PYROLYSIS

Coal pyrolysis is an initial step in the coal thermal decomposition process and plays an important role in coal-based direct reduction of iron ore. In the initial stages of reduction, the compounds that evolve from the coal (and later, these together with the products of the Boudouard and water gas reactions) provide the reductant for the iron ore. When volatile materials reach the outside of a specimen, they reduce the reoxidation potential of the outer atmosphere and provide heat as they burn. During pyrolysis, the structure of the coal changes and becomes more porous. This increases the rate of production of reductants through the Boudouard and water gas reactions and decreases the thermal conductivity of the pellet. The final degree of reduction increases with increasing volatile-matter content.[58] The presence of volatile matter in coal increases the speed of the metallization process and raises the melting temperature of the resultant sponge iron.[9]

The presence of iron oxides affects the coal thermal transformation and, hence, coal pyrolysis.[59–63] Haque et al.[59] (tests at 600 °C) showed that in the presence of Fe_2O_3 the yield of tar decreases, and Lasarev and Chlebik[60] showed an increase in the formation of water. Cypres and Soudan–Moinet[62] showed that the presence of iron oxides reduces the primary devolatilization rate of coal between 300 °C and 600 °C, so the yields of tar and hydrocarbon decrease. In the secondary devolatilization zone, the production of CO, H_2O, and CH_4 increases in the presence of iron oxides, while the hydrogen yield decreases.

The modeling of coal pyrolysis is a challenging task in itself, even for pure coal when it is not mixed with iron ore.[64–71] The simplest model for the evolution of the total amount of volatiles produced up to time t (or for modeling the evolution of individual species) is the first-order reaction model:

$$\frac{dV}{dt} = k(V^* - V) \qquad [42]$$

where V is the mass fraction of volatiles evolved up to time t and V^* is the value of V as $t \to \infty$. The rate constant k typically has the Arrhenius form (Eq. [12]). Sun and Lu[46,47,48] use this model, and parameters for the modeling of the evolution of different species are taken from early work by Solomon and Colket[72] (Eqs. [44] through [50]).

$$k_{TAR} = 750 \exp\left(-8000/T\right) \qquad [43]$$

$$k_{HHC} = 4200 \exp\left(-9000/T\right) \qquad [44]$$

$$k_{CO_2} = 6 \exp\left(-4000/T\right) \qquad [45]$$

$$k_{H_2O} = 15 \exp\left(-4950/T\right) \qquad [46]$$

$$k_{CO-L} = 7000 \exp\left(-10,300/T\right) \qquad [47]$$

$$k_{LHC} = 2300 \exp\left(-9700/T\right) \qquad [48]$$

$$k_{H_2} = 3600 \exp\left(-12,700/T\right) \qquad [49]$$

$$k_{CO-T} = 890 \exp\left(-12,000/T\right) \qquad [50]$$

In Solomon and Colket's devolatilization model, the coal is assumed to consist of nonvolatile carbon (NVC) and abstracted hydrogen by tar (AH) plus the sources for the following light-volatile components: CO_2, tightly bound CO (CO-T), H_2O, loosely bound CO (CO-L), light hydrocarbons (LHC), heavy hydrocarbons (HHC), and H_2. It is assumed that evolution of the light-volatile components occurs simultaneously with tar and that the evolving tar has the same composition as the coal. As the authors state: "The heated coal can be pictured as a soup in which some of the ingredients evaporate (the light-volatile components) while, at the same time, the soup is being ladled out. The composition of the ladled-out soup (the tar) and the remaining soup (the char) will change as the ingredients evaporate." Solomon and Colket found that even though the amount of each component is different in different coals, the rates of evolution are relatively independent of coal type. In that article, they found that this result did not hold for CO, but in later investigations[66,67] it did hold for CO as well, when the multiple-reaction model was applied and CO evolution was subdivided into more components: CO—ether loose, CO—ether tight, and CO—extra tight.

Different authors (for example, Solomon et al.[66] and Anthony et al.[73]) have shown that for devolatilization of coal, the values of k_0 and E determined for one heating rate are not applicable when used for another heating rate. For modeling reduction in large specimens, heat transfer should be taken into account, so the change of temperature cannot be described with an overall uniform heating rate.

Currently, the most frequently used model for simulating evolution of different species from coal during its thermal decomposition is the multiple-reaction model with distributed activation energies, also called the distributed activation-energy model (DAEM).[64,65,70,71]

Here, the DAEM description follows the description in work by Donskoi and McElwain.[70] This model assumes that the evolution of a certain substance involves an infinite number of independent chemical reactions. The contribution to evolution by a particular reaction is described in a manner similar to Eq. [42], that is,

$$\frac{dV_i}{dt} = k_i(V_i^* - V_i) \qquad [51]$$

where i denotes one particular reaction called a "sample reaction." The mass of volatiles released for one sample reaction is obtained by integration of Eq. [51], namely,

$$V_i = V_i^* - V_i^* \exp\left(-\int_0^t k_i dt\right) \qquad [52]$$

It is assumed that the k_i terms are given by Arrhenius expressions (Eq. [12]), and it is also assumed that they dif-

fer only in activation energy and that the number of reactions is large enough to permit the distribution of energy to be expressed as a function $f^*(E)$, where $V^*f^*(E)dE$ represents the fraction of the potential volatile loss (V^*) that has an activation energy between E and $E + dE$. Thus, the total amount of volatile material released up to time t is given by

$$V = V^* - V^* \int_0^\infty \exp\left(-\int_0^t k(E)dt\right) f^*(E)dE \quad [53]$$

The distribution $f^*(E)$ is taken to be a Gaussian distribution with a mean activation energy (E_0) and standard deviation (σ). Assuming that $k(E) = k_0 \exp(-E/RT)$, expression [53] becomes

$$V^* - V = \frac{V^*}{\sigma(2\pi)^{1/2}} \int_0^\infty \exp\left(-k_0 \int_0^t \exp(-E/RT)dt\right. \\ \left. - \frac{(E - E_0)^2}{2\sigma^2}\right) dE \quad [54]$$

In later work,[67,74] Solomon *et al.* further developed a devolatilization model where more components and the DAEM were introduced. All kinetic parameters for the later model can be found in Solomon *et al.*[66,67]

As can be seen from expression [54], in a system in which the temperature varies from point to point, the computations become very expensive, since they require the evaluation of a complicated double integral at every point in space at every time step. A special numerical method (the modified Gauss–Hermite quadrature (MGHQ)) for integrating the DAEM has been developed by Donskoi and McElwain.[71] It permits a significant reduction in the computation time in comparison with the standard approaches. Also, the MGHQ permits easy predictions of the calculation error, while for standard methods, analytical estimation of the error is almost impossible.

To avoid the DAEM integration, Donskoi and McElwain proposed an nth-order reaction model[70] which approximates the DAEM quite well. In this model, the evolution of a certain component is modeled as an nth-order reaction for a certain range of heating rates and is expressed as

$$\frac{dV}{dt} = k_0 \exp(-E_A/RT)(V^* - V)^n \quad [55]$$

Here, n is the "order" of the reaction. For modeling processes with quite a large range of heating rates, differing by 20 to 40 orders in magnitude, the formulae for k_0 and E_A are simple functions of the heating rate m:

$$k_0 = A + B m \quad [56]$$

$$E_A = C + D \ln(m) \quad [57]$$

where A through D are constants. These coefficients and the parameter n can be found from an experiment or from data for the MRM. Donskoi and McElwain[70] calculated all the coefficients for the nth-order model for the coal-independent set of kinetic parameters of the DAEM, based on an approach given by Solomon *et al.*[66,67] As shown in their article,[70] the approximate nth-order reaction model fits the DAEM solution quite well.

IV. CONCLUSIONS

Different approaches to modeling kinetic parameters like the rates of reduction, gasification, and devolatilization in DRIOCC have been critically analyzed. The review of the modeling of the rate of reduction has shown that quite different techniques, from regression analyses to detailed mathematical descriptions, can be applied to model experimental data. It is concluded that the time course of the reduction can be simulated without developing detailed mechanisms for the chemical reactions and heat and mass transfer. However, if the specifics of gas production, concentration of particular species, or physical properties such as the thermal conductivity are required, then a more detailed model needs to be developed. The modeling technique adopted should depend on the experimental conditions like specimen and particle sizes, ambient atmosphere, heating regimes, geometry, and composition. To reflect the dependence of the pyrolysis kinetic parameters on heating regimes, more-comprehensive methods than the first-order reaction modeling should be applied. The nth-order reaction modeling and MGHQ method developed by the authors permit a significant reduction in the computation time in comparison with the standard distributed activation-energy approach.

APPENDIX

Equilibrium constants

Equilibrium constants for Reactions [1], [3], and [5] can be taken from the study by Omori,[75] and for temperatures under 848 K, they are

$$K_1 = \exp(4.91 + 6235/T) \quad \text{for } f < 0.111 \quad [A1]$$

$$K_{3,5} = \exp(-0.7625 + 543.3/T) \quad \text{for } f > 0.111 \quad [A2]$$

For temperatures over 848 K:

$$K_1 = \exp(4.91 + 6235/T) \quad [A3]$$

$$K_3 = \exp(2.13 - 2050/T) \quad [A4]$$

$$K_5 = \exp(-2.642 + 2164/T) \quad [A5]$$

Equilibrium constants for Reactions [2], [4], and [6] can be taken from work by Miyasaka *et al.*,[76] and for temperatures under 848 K, they are

$$K_2 = \exp(8.384 + 2546.5/T) \quad \text{for } f < 0.111 \quad [A6]$$

$$K_{4,6} = \exp(2700 - 3183/T) \quad \text{for } f > 0.111 \quad [A7]$$

For temperatures over 848 K:

$$K_2 = \exp(8.102 + 2065/T) \quad [A8]$$

$$K_4 = \exp(2.13 - 2050/T) \quad [A9]$$

$$K_6 = \exp(-2.642 + 2164/T) \quad [A10]$$

The equilibrium constant for the Boudouard reaction can be taken from work by Esdale and Motlagh:[77]

$$K_B = \exp(21.0 - 20{,}546.5/T) \quad [A11]$$

The equilibrium constant for the carbon gasification water gas reaction has been calculated from data for the standard Gibbs free-energy change given by Gaskel:[78]

$$K_{wg} = \exp\left(17.2684 - 16{,}341.8/T\right) \qquad [A12]$$

For detailed equilibrium diagrams for direct reduction of iron ore, an excellent source is the articles by Esdale and Motlagh.[77,79,80]

ACKNOWLEDGMENTS

REFERENCES

1. E. Donskoi and D.L.S. McElwain: *Ironmaking and Steelmaking*, 2001, vol. 28 (5), pp. 1-6.
2. S. Sun: Ph.D. Thesis, McMaster University, Hamilton, On, Canada, 1997.
3. P.C. Ghosh and S.N. Tiwari: *J. Iron Steel Inst.*, 1970, vol. 208, pp. 255-57
4. Y.K. Rao: *Metall. Trans.*, 1971, vol. 2, pp. 1439-47.
5. R. Fruehan: *Metall. Trans. B*, 1977, vol. 8B, pp. 279-86.
6. N.S. Srinivasan and A.K. Lahiri: *Metall. Trans. B*, 1977, vol. 8B, pp. 175-78.
7. C. Seaton, J. Foster, and J. Velasco: *Trans. Iron Steel Inst. Jpn.*, 1983, vol. 23, pp. 490-96.
8. K. Otsuka and D. Kunii: *J. Chem. Eng. Jpn.*, 1967, vol. 2, pp. 46-50.
9. C. Bryk and W.-K. Lu: *Ironmaking and Steelmaking*, 1986, vol. 13, pp. 70-75.
10. S. Prakash and S. Ray: *Iron Steel Inst. Jpn. Int.*, 1990, vol. 30 (3), pp. 183-91.
11. G. Reddy, T. Sharma, and S. Chakravorty: *Ironmaking and Steelmaking*, 1991, vol. 18 (3), pp. 211-13.
12. S. Mookherjii, H.S. Ray, and A. Mukherjee: *Ironmaking and Steelmaking*, 1986, vol. 13, pp. 229-35.
13. R. Haque, H.S. Ray, and A. Mukherjee: *Ironmaking and Steelmaking*, 1992, vol. 19 (1), pp. 31-35.
14. R. Nascimento, M. Mourao, and J. Capocchi: *Ironmaking and Steelmaking*, 1999, vol. 26 (3), pp. 182-86.
15. Q. Wang, Z. Yang, J. Tian, W. Li, and J. Sun: *Ironmaking and Steelmaking*, 1998, vol. 25, pp. 443-47.
16. S. Prakash: *J.S. Afr. Inst. Mining Metall.*, 1996, vol. 96 (1), pp. 3-16.
17. S.K. Dey, B. Jana, and A. Basumallick: *Iron Steel Inst. Jpn. Int.*, 1993, vol. 33, pp. 735-39.
18. Q. Wang, Z. Yang, J. Tian, W. Li, and J Sun: *Ironmaking and Steelmaking*, 1997, vol. 24, pp. 457-60.
19. S.K. Dutta and A. Ghosh: *Metall. Trans. B*, 1994, vol. 25B, pp. 15-26.
20. R. Carvalho, P. Netto, and L. D'Abreu: *Can. Met. Q.*, 1994, vol. 33, pp. 217-25.
21. A. Ghosh, M.N. Mungole, G. Gupta, and S. Tiwari: *Iron Steel Inst. Jpn. Int.*, 1999, vol. 39 (8), pp. 829-31.
22. S. Prakash: *Ironmaking and Steelmaking*, 1994, vol. 21 (3), pp. 237-43.
23. R. Haque and H. Ray: *Metall. Trans. B*, 1995, vol. 26B, pp. 400-01.
24. A.M. Chernyshev, N.K. Karnilva, and Y.V. Tarasenko: *Steel USSR*, 1979, vol. 7 (3), pp. 133-35.
25. O.G. Dam Gonzales and J.H.E. Jeffes: *Ironmaking and Steelmaking*, 1987, vol. 14, pp. 217-22.
26. W.M. McKewan: *Trans. TMS-AIME*, 1960, vol. 2, pp. 2-6.
27. J. Szekely, J.W. Evans, and H.Y. Sohn: *Gas-Solid Reactions*, Academic Press, New York, NY, 1976.
28. G. McAdam, D. O'Brien, and T. Marshall: *Ironmaking and Steelmaking*, 1977, vol. 1, pp. 1-9.
29. W. Baukloh and R. Durrer: *Arch. Eisenhuttenwes.*, 1931, vol. 4, pp. 455-60.
30. T.S. Yun: *Trans. ASM*, 1961, vol. 54, pp. 129-42.
31. S. Prakash and S. Ray: *Thermochimica Acta*, 1987, vol. 111, pp. 143-46.
32. B. Huang and W. Lu: *Iron Steel Inst. Jpn. Int.*, 1993, vol. 33, pp. 1055-61.
33. A.F. Armington: Ph.D. Thesis, The Pennsylvania State University, University Park, PA, 1960.
34. S. Ergun: *J. Phys. Chem.*, 1956, vol. 60, p. 480.
35. E.T. Turkdogan, V. Koump, J.V. Vinters, and T.F. Perzak: *Carbon*, 1968, vol. 6, pp. 462-84.
36. P.L. Walker, Jr., M. Shelef, and R.A. Anderson: *Chem Phys. Carbon*, 1968, vol. 4, pp. 287-383.
37. H. Ohme and T. Suzuki: *Energy and Fuels*, 1996, vol. 10 (4), pp. 980-87.
38. T. Kodama, A. Funatoh, K. Shimizu, and Y. Kitayama: *Energy Fuels*, 2001, vol. 15 (5), pp. 1200-06.
39. E.T. Turkdogan and J.V. Vinters: *Carbon*, 1972, vol. 10, pp. 97-111.
40. F.J. Long and K.W. Sykes: *J. Chem. Phys.*, 1950, vol. 47, p. 361.
41. R. Haque, H.S. Ray, and A. Mukherjee: *Scand. J. Metall.*, 1992, vol. 21, pp. 78-85.
42. L. von Bogdandy and H.J. Engell: *The Reduction of Iron Ores*, Springer-Verlag, Berlin, 1971.
43. C. Seaton, J. Foster, and J. Velasco: *Trans. Iron Steel Inst. Jpn.*, 1983, vol. 23, pp. 497-503.
44. E.M. Donskoi, F. Liu, and D.L.S. McElwain: *Computational Techniques and Applications: CTAC97*, World Scientific Publishing Co., Singapore, 1998, pp. 193-200.
45. E.M. Donskoi, D.L.S. McElwain, and F. Liu: *Proc. Aus. Engineering Mathematics Conf. AEMC96*, Sydney, 1996, pp. 79-84.
46. S. Sun and W. Lu: *Iron Steel Inst. Jpn. Int.*, 1993, vol. 33, pp. 1062-69.
47. S. Sun and W.-K. Lu: *Ironmaking Conf. Proc.*, 1996, vol. 55, Pittsburgh, PA, Iron and Steel Society, Warrendale, PA, pp. 645-52.
48. S. Sun and W. Lu: *Iron Steel Inst. Jpn. Int.*, 1999, vol. 39 (2), pp. 123-29, and pp. 130-138.
49. D.D. Do: *Chem. Eng. Sci.*, 1982, vol. 37, pp. 1477-81.
50. T. Usui, M. Ohmi, S. Hirashima, and Oshima: *Proc. 6th Process Technology Conf.*, 5th *Int. Iron and Steel Congr.*, Washington, 1986, D.C., pp. 545-53.
51. M. Ohmi, T. Usui, Y. Minamide, and M. Naito: *Proc. 3rd Int. Iron and Steel Congr.*, Metals Park, OH, 1979, pp. 472-78.
52. M.A.M. Boersma, J.A.M. Spiers, and H.S. Van der Bann: *Chem. Eng. Sci.*, 1980, vol. 35, pp. 1237-43.
53. M.P Dudukovic and H.S. Lamba: *Chem. Eng. Sci.*, 1978, vol. 33, pp. 303-14.
54. W.E. King, Jr. and W.S. Jones: *Chem. Eng. Sci.*, 1979, vol. 34, pp. 1387-92.
55. S.K. Bhatia and D.D. Perlmutter: *AIChE J.*, 1980, vol. 26, pp. 379-86.
56. S.K. Bhatia and D.D. Perlmutter: *AIChE J.*, 1981, vol. 27, pp. 247-54.
57. S.K. Bhatia and B.J. Vartak: *Carbon*, 1996, vol. 34, pp. 1383-91.
58. T. Sharma: *Ironmaking and Steelmaking*, 1993, vol. 20, pp. 362-65.
59. R. Haque, G.J. Lawson, and S.G. Ward: *6th Int. Congr. on Coal-Munster*, 1965.
60. I. Lasarev and A.F. Chlebik: *Prace Ustavu Vyzkum Paliva*, 1960, vol. 3, p. 77.
61. H. Barking and C. Eymann: *G.W.F. (Gas)*, 1958, vol. 99 (41), p. 1037.
62. R. Cypres and C. Soudan-Moinet: *Fuel*, 1980, vol. 59, pp. 48-54.
63. R. Cypres and C. Soudan-Moinet: *Fuel*, 1981, vol. 60, pp. 33-39.
64. D.B. Anthony, J.B. Howard, H.C. Hottel, and H.P. Meissner: *Fuel*, 1976, vol. 55, pp. 121, *Fuel*, 1976, vol. 55, pp. 121-28.
65. J.B. Howard: in *Chemistry of Coal Utilization*, 2nd Suppl. Vol., M.A. Elliott, ed., John Wiley & Son, New York, NY, 1981, ch. 12.
66. P.R. Solomon, M.A. Serio, and E.M. Suuberg: *Progr. Energy Combust. Sci.*, 1992, vol. 18, pp. 133-220.
67. P. Solomon, D. Hamblen, R. Carangelo, M. Serio, and G. Deshpande: *Energy Fuels*, 1988, vol. 2, pp. 405-22.
68. S. Niksa and C.W. Lau: *Combust. Flame*, 1993, vol. 94, pp. 293-307.
69. J.C. Chen: *Combust. Flame*, 1996, vol. 107, pp. 291-98.
70. E. Donskoi and D.L.S. McElwain: *Fuel*, 1999, vol. 78, pp. 825-35.
71. E. Donskoi and D.L.S. McElwain: *Combust. Flame*, 2000, vol. 122, pp. 359-67.

72. P.R. Solomon and M.B. Colket: *17th Symp. (Int) on Combustion*, The Combustion Inst., Pittsburgh, PA, 1978, pp. 131-43.
73. D.B. Anthony, J.B. Howard, H.C. Hottel, and H.P. Meissner: *15th Symp. (Int.) Combustion*, Combustion Institute, Pittsburgh, PA, 1975, pp. 1303-17.
74. P.R. Solomon, D.G. Hamblen, M.A. Serio, Z.Z. Yu, and S. Charpenay: *Fuel*, 1993, vol. 72, pp. 469-88.
75. Y. Omori: *Blast Furnace Phenomena and Modeling*, Elsevier Applied Science, London, 1987, pp. 97-280.
76. N. Miyasaka, M. Sugata, Y. Hara, and S. Kondo: *Trans. Iron Steel Inst. Jpn.*, 1975, vol. 15, pp. 27-36.
77. J. Esdale and M. Motlagh: *Ironmaking and Steelmaking*, 1991, vol. 18, pp. 423-30.
78. D.R. Gaskell: *Introduction to the Thermodynamics of Materials*, Taylor & Francis, Washington, DC, 1995, p. 544.
79. M. Motlagh: *Ironmaking and Steelmaking*, 1992, vol. 19, pp. 469-78.
80. M. Motlagh: *Iron Steelmaker*, 1994, vol. 21, pp. 75-82.